JOURNAL OF Materials CHEMISTRY

A study of impurities in some CdS/CdTe photovoltaic cells prepared by wet-chemical methods using secondary ion mass spectrometry and X-ray photoelectron spectroscopy

David S. Boyle,[a] Sean Hearne,[b] Daniel R. Johnson[c] and Paul O'Brien*†[a]

[a]*Department of Chemistry, Imperial College of Science, Technology and Medicine, South Kensington, London, UK SW7 2AZ. E-mail: p.obrien@ic.ac.uk*
[b]*National Microelectronics Research Centre (NMRC Ireland), University College, Lee Malting, Prospect Row, Cork, Ireland*
[c]*BP Solar Ltd, Unit 12 Brooklands Close, Sunbury-on-Thames, Middlesex, UK TW16 7DX*

Received 11th June 1999, Accepted 3rd September 1999

Quantitative Secondary Ion Mass Spectrometry has been used to determine the elemental profiles and concentrations of isotopes ^{12}C, ^{16}O, ^{34}S and ^{35}Cl within n-CdS/p-CdTe thin film photovoltaic cells. Chemical Bath Deposition (CBD) was used to deposit the CdS window layers. The annealing process induces the formation of a chloride-rich surface layer on CdS as evidenced from X-ray photoelectron spectroscopy measurements. The carbon impurity in heterostructures appears to influence the chloride-promoted recrystallisation of CdTe. High concentrations of ^{16}O, of the order 10^{20}–10^{21} atoms cm^{-3} throughout the cells, are consistent with the formation of oxide material in the post-deposition thermal processing. Isotopic profiles for ^{12}C, ^{34}S and ^{35}Cl have similar maxima ($\approx 10^{19}$ atoms cm^{-3}) but concentrate at the CdS–CdTe interface. The relatively high tolerance to high concentrations of impurities in our cells suggests that wet chemical methods may have great potential in the fabrication of large area/low cost devices.

Introduction

Thin film n-CdS/p-CdTe solar cells have been demonstrated to be potentially efficient and economically attractive photovoltaic devices. The BP Solar 'Apollo' cell uses this configuration.[1] Understanding the complex parameters controlling heterojunction formation and interfacial properties, with respect to synthetic methodology, is crucial in further developing such devices for commercial manufacture. Such polycrystalline thin film solar cells are most efficient in the heterojunction configuration. Two semiconductors of opposite conductivity type, a 'window' layer and an 'absorber' layer (in which E_{g1} of the window material $> E_{g2}$ bandgap of absorber material), are used to form a p–n junction. There are many reviews and books that describe the technology.[2] The main advantage of heterojunction thin film solar cells is their promise as low cost alternatives to devices based on silicon.

The Chemical Bath Deposition (CBD) of compound semiconductors has recently attracted interest,[3] because the technique offers many advantages over the more established synthetic routes to semiconductor materials.[4] Factors such as control of film thickness and deposition rate by varying pH, solution temperature and reagent concentration are allied with a potential to coat large area, in a reproducible and low cost process. In addition, the homogeneity and stoichiometry of the product are maintained partly by the solubility product (K_{sp}) of the material in question.[5]

It has been established that solar cell efficiencies are sensitive to the nature of the CdS–CdTe interface.[6] The optimisation of each layer in a device depends on the processing of the adjacent layers. The effects of high temperature processing (either during deposition or after film growth) and $CdCl_2$ treatments on the performance of the device are widely reported[7] but poorly understood. Moreover, the importance of CdS–CdTe interdiffusion and O and Cl doping (either deliberate or as a consequence of the method of synthesis) have yet to be established quantitatively.

Chloride treatment and annealing are associated with the promotion of grain growth and interdiffusion in CdTe–CdS layers. The treatment changes the current transport mechanism from interface recombination and tunneling to a thermally activated process. The behaviour is consistent with a decrease in the importance and concentration of interface states.[8] Passivation of grain boundaries *via* chloride treatment is also consistent with the observed high cell efficiencies. It has been reported that low efficiency cells possess near stoichiometric or Cd-rich CdTe surfaces and abrupt heterointerfaces, while higher efficiency cells are characterised by Te-rich CdTe and smooth interfaces.[6]

In the present work we have started to investigate quantitatively, for the first time, the concentrations of chemical impurities found in cells fabricated by 'wet-chemical' methods. These methods produce devices with acceptable efficiencies from processes radically different from techniques such as close space sublimation (CSS) or chemical vapour deposition (CVD). There may be relationships between some impurities in layers and their distribution and the relatively high cell efficiencies of chemically processed cells.[9]

The technique of Secondary Ion Mass Spectrometry (SIMS) involves the detection of charged secondary ions, produced as a result of sputtering of a substrate surface by energetic primary ions. The approach appears well suited to the study of such photovoltaic cells.[10] In dynamic SIMS the primary ion density is sufficient to erode the surface, hence depth profiling of elements (with isotopic discrimination) is possible. However, the quantification of SIMS data is difficult as the measured secondary ion flux is not easily related to the concentration of the particular ion in the solid. The use of ion-implanted standards does make it possible to derive a relative sensitivity factor (RSF) for the particular isotope of interest. This approach allows the calculation of concentrations in deposited

†Present address: The University of Manchester, Department of Chemistry, Oxford Road, Manchester, UK M13 9PL.

layers from ion intensity data. In depth profiling SIMS the characteristic ions are monitored as a function of time. A profilometer is subsequently used to determine the depth of the crater produced by ion sputtering (assuming a flat bottomed pit), hence the isotopic concentration profile through a sputtered sample may be determined.

In this work we have determined the concentration profiles for some significant impurities in functional CdS/CdTe photovoltaic cells, synthesized by wet-chemical methods. Four different chemical baths have been used to deposit the CdS layer, in an attempt to see if variance in bath chemistry leads to differences in composition of heterostructures in the final cell.

Experimental

The deposition of CdS by CBD and electrodeposition of CdTe layers

The CdS thin films ($\approx$80 nm) were grown on commercial tin oxide glass substrates (TEC 10, Libby-Owens Ford) from four different chemical bath solutions containing a cadmium salt, an amine complexant(s), thiourea and sodium hydroxide to obtain a solution of final pH$\approx$10.5–12 (Table 1). An EIL 7000 pH meter with temperature compensation and Russell glass electrode (calibrated against standard pH 7.00 and 10.00 buffers) were used to record solution pH. Substrates were degreased and cleaned thoroughly by ultrasonication in a standard procedure before immersion in the chemical bath. The reaction mixture was mechanically stirred and maintained at the appropriate temperature (343–353 K) for deposition. Substrates were removed from the bath after the desired period of time, washed with de-ionised water and any adherent particulate matter was removed by ultrasonic agitation. The substrates were allowed to dry and subsequently annealed in air.

The electrodeposition of CdTe has been reported elsewhere[11] and involves the formation of CdTe layers ($\approx$1700 nm) from an aqueous solution containing Cd^{2+} and $HTeO^{2+}$ ions. The as-deposited CdTe layers exhibit n-type conductivity; a post-deposition heat treatment is employed to effect type conversion and produce an efficient p–n junction. Both CdS and CdTe were doped with Cl in this work, as this has been shown to have a beneficial effect in promoting grain growth and intermixing of CdS and CdTe.[12]

XPS, UV-vis and cell characterisation

Compositional analysis of the CdS films was performed before and after air annealing using X-Ray Photoelectron Spectroscopy (XPS). The XPS measurements were conducted in the ultra-high vacuum chamber (base pressure 10^{-8} Pa) of a VG ESCALAB-Mk II (VG Scientific) using Al-Kα excitation (analyser pass energy of 50 eV). The energy scale was calibrated using C_{1s} (at 284.8 eV) as a reference. Electronic absorption spectra were recorded with a Philips PU 8710 spectrophotometer. Film thicknesses were calculated from transmission/reflection measurements made using a Mono-light system at BP Solar Ltd. A standard process employed by BP Solar[1] was used for the fabrication of photovoltaic modules (100×100 mm) from 300×300 mm substrates. Device efficiencies were determined by *I–V* analysis of *ca.* 0.1 cm^2 areas under near AM 1.5 conditions ($\approx$100 mW cm^{-2} illumination using ELH lamps behind diffusing glass). The spectral response of cells was measured under white light bias (40 mW cm^{-2}) from 350 to 900 nm with applied bias.

Analysis by quantitative secondary ion mass spectrometry (SIMS)

Back contacts (Au) were removed by delamination. The CdTe layers presented smooth surfaces (root-mean-square (RMS) values *ca.* 50–60 Å as determined by a Dektak profiler) for SIMS analysis. A standard CAMECA IMS 3f Ion Microscope with gas duoplasmatron (argon and oxygen) and Cs^+ (13 keV impact energy) primary ion sources was utilised, with a Sun SPARC station data acquisition and processing system and CAMECA IMS software. Ion-implanted samples of polished CdTe (obtained commercially from AEA Technology) containing the isotopes ^{16}O, ^{34}S, ^{35}Cl, ^{12}C and ^{14}N were prepared. The position of the elements in the Periodic Table made the choice of Cs^+ bombardment most appropriate. The dose method was employed to calculate the RSF values (as the direct concentration method is highly dependent on the precise measurement of secondary ion intensity at a given depth of ion-implanted sample and is less easily determined) and the following relationship was used to relate the parameters:

$$\mathrm{RSF} = D\int(I/I_{\mathrm{ref}}) \quad (1)$$

RSF is the relative sensitivity factor, D the specific ion-implantation dose in the host matrix to yield a Gaussian distribution, I the recorded secondary ion intensity and I_{ref} the secondary ion intensity recorded for the reference element in the ion-implanted standard. A full elemental profile for each sample was taken in order to establish the nature of any isotopic interferences (*e.g.* for the element chlorine, the ratio of secondary ion intensities for nominal mass 35 [^{35}Cl] and 37 [^{37}Cl] was consistent with that expected). The presence of the SnO_2/F layer on the glass substrate material provided both an antidiffusion layer and means by which the termination of the CdS layer was determined.

The post analysis calibration of the depth scale for each SIMS analysis was achieved with a TENCOR Alfa-step stylus surface profiler. In order to establish the reproducibility of our experimental arrangement a total of 5–10 SIMS profiles were recorded for each sample. The sputter craters possessed flat bottomed surfaces and the etch rates through the entire cell structure of all samples were relatively constant, hence the average sputter rate was calculated in terms of the crater depth and total sputter time. The ion intensity scale was converted into concentration by application of the appropriate relative sensitivity factors (Table 2).[13]

Results and discussion

XPS studies

It is widely known that CBD produces films with a relatively high concentration of impurities (*ca.* 0.1–1 mole%).[14] The use of XPS as an analytical technique[15] for surfaces is common,

Table 1 Composition of chemical baths used for the deposition of CdS films

	Concentration/mmol dcm^{-3}				
Bath no.	Cadmium	NaOH	Ammonia	1,2-Diaminoethane	Thiourea
1	2.0	14.5	250	6.0	2.46
2	3.0	9.2	250	8.7	2.46
3	2.0	14.5	0	6.0	2.46
4	2.0	5.2	0	6.0	7.66

Table 2 Ion implant parameters of polycrystalline CdTe standards employed during SIMS study

Ion implant	10^{-3} Crater depth/nm	Sputter rate/nm s^{-1}	Relative sensitivity factor (RSF) $\times 10^{17}$
Carbon-12	4.9	1.673	3.01
Oxygen-16	4.9	1.11	0.558
Sulfur-34	4.9	1.22	0.162
Chlorine-35	4.9	1.33	0.373

Table 3 Photoelectron binding energies (eV) and peak assignments for as-deposited and heat-treated CBD CdS films. Data compared with values obtained from ref. 15

Photoelectron peak	Standard[a]	CdS (as deposited)	CdS (heat treated)
Cd $3d_{5/2}$	405	405.1	405.1
Cd $3d_{3/2}$	412	411.9	411.9
Cd(Auger)	1105/111	1105.2/1111.2	1105.0/1111.5
S 2p	162	162.0	162.0
N 1s	400	395.7	
O 1s	531	531.9	
Cl 1s	285	284.8	282.8
Na 1s	1072		1071.5
Cl $2p_{3/2}$	199		199.5

[a]All elements are confirmed as being present in 'normal' oxidation states.[15]

although the spatial resolution ($\approx$0.2 mm) is relatively poor. Non-equivalent atoms of the same element in a solid should give rise to core-level peaks with measurably different binding energies. We have carried out XPS measurements to give some possibility for direct composition of our CBD CdS to those reported by other workers on similar CdS films.[16] Carbon, nitrogen and oxygen were detected as impurities in the as-deposited films (Table 3).

Upon the annealing of films in air, the nitrogenous contaminant is reduced to a concentration below the detection limit of the instrument. The effect is probably due to the evaporation of ammonia or ethylenediamine, occluded during deposition, from the films. Concurrently the chloride species becomes observable in the XPS spectrum at 199.5 eV (Cl $2p_{3/2}$). Similar observations have been made by ourselves and others employing the SIMS technique[9] and/or XPS.[17] The presence of a chloride-rich layer on CdS has been associated with efficient type conversion of CdTe layers upon annealing of heterojunction devices.[18] In addition, a peak at 1071.5 eV was found to develop for heat-treated CdS films which was assigned to Na 1s photoelectrons. The annealing process in air does not appear to degrade the CdS films. No signals typical of the products of oxidation, *e.g.* 168.7 eV (S 2p for SO_4^{2-}),[17] were observed. Owing to the broad nature of the O 1s peak, the feature may represent several chemically or physically bound water or hydroxide molecules at the surface.[18]

SIMS studies

For all samples it was observed that steady-state sputtering conditions were reached at a depth *ca.* 150 nm into the material (Fig. 1A–1D). A recent study[19] suggests that concentration calibration, based upon the assumption of a constant ion yield ratio or a constant relative sensitivity factor (RSF), may be capricious in the region of transition. However, there is no serious problem as the etch rate across the device was observed to be constant (*ca.* 1.5 mm s^{-1}) through the CdTe/Cd(Te,S)/CdS layers of the cell (Table 4). Initial efforts revealed that the low negative secondary ion yield of nitrogen would not allow the collection of accurate and reproducible data. Hence only the isotopic profiles for ^{16}O, ^{34}S, ^{35}Cl and ^{12}C were determined. The SIMS ^{14}N depth profiles in CBD CdS layers have been reported by other workers but the results were not quantitative.[9]

The very high concentrations of detected oxygen, carbon and chlorine made it necessary to establish whether the signals were due to real impurities in the sample, or artifacts due to instrumental memories from previous analysed material. The impurity intensity was measured for each sample with different raster sizes and constant primary beam current. It was found that the impurity signal intensities were proportional to the sputtering rate, therefore the source of the oxygen, carbon and chlorine was not artifactual.

The concept of accurate depth profiling of any given species assumes that it is possible to determine the original location of the species. For the SIMS technique there are several processes that may operate concurrently and complicate the interpretation of isotopic profiles. The most significant are radiation and bombardment induced material transport, elemental-differential sputtering, collisional mixing and radiation-enhanced diffusion. These factors are discussed in detail elsewhere.[20] In addition, dopant diffusion coefficients are greatly enhanced at grain boundaries, so on a microscopic level we may expect to observe highly non-uniform depth profiles for impurities in the cell structures. The large differences in the sputtering yields of randomly orientated crystals in polycrystalline samples result in different erosion rates for individual grains. This effect results in a progressive roughening of the eroded surface. In order to obtain good depth profiles for polycrystalline samples we require ion bombardment conditions that minimise roughening of the eroded surface, as the effect usually generates a more pronounced broadening effect than bombardment induced atomic mixing. The interpretation of SIMS profiles in our study was convincing as we observed flat bottomed etch pits.

For all the CdS/CdTe photovoltaic cells in this study the general patterns of isotopic distributions from SIMS analysis were similar. The relative concentrations followed the order $^{16}O > ^{35}Cl > ^{12}C > ^{34}S$ through the main body of the CdTe matrix. It is known that CdTe has a propensity for self-compensation, hence the effective dopant concentration may

Table 4 The sputtering parameters determined for CdS/CdTe samples. Figures given for the erosion rates apply to the bulk matrix for which steady-state sputter conditions were established

Sample	Crater depth/nm	Sputter rate/nm s^{-1}
1	1.89	1.62
2	1.88	1.73
3	1.84	1.56
4	2.10	1.56

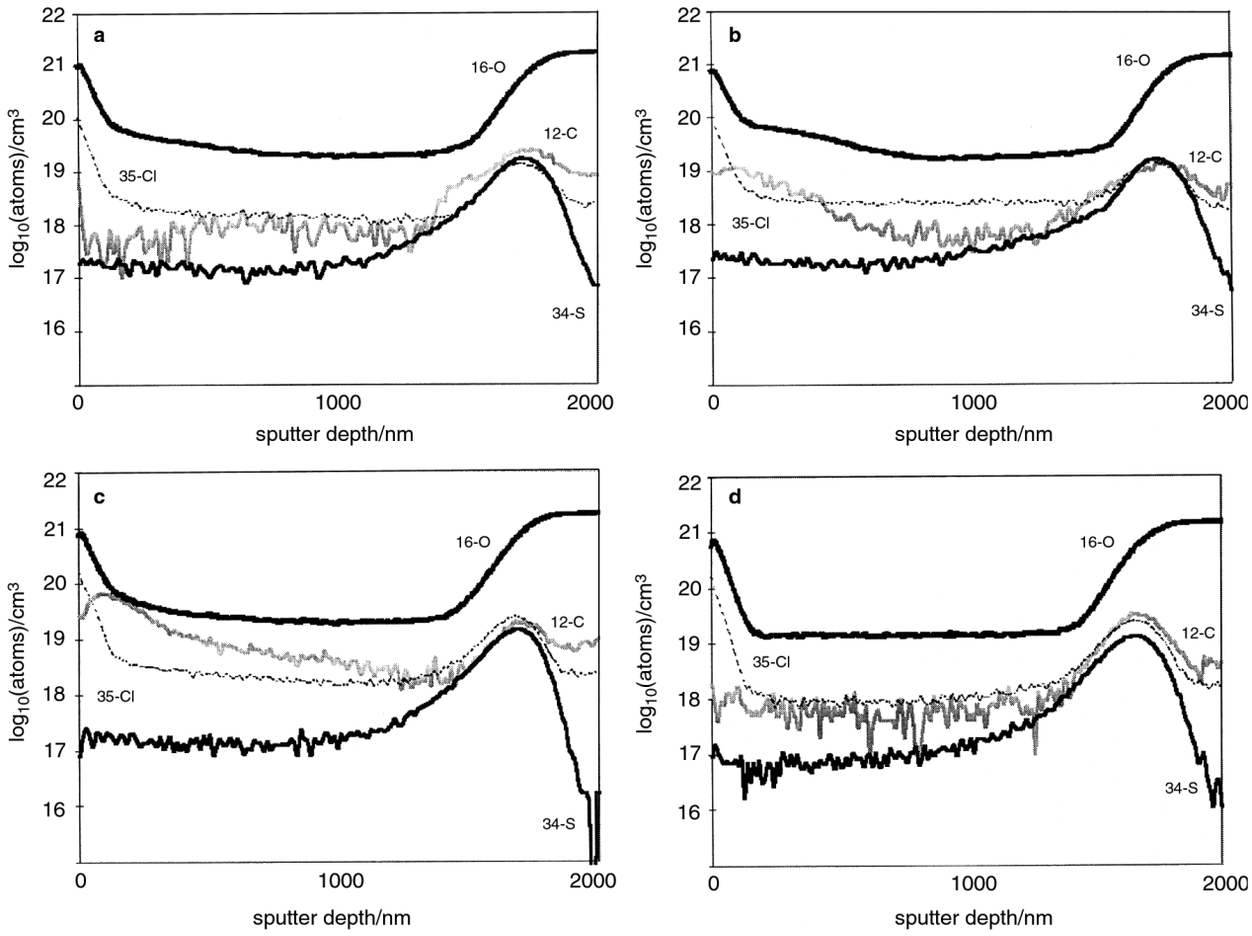

Fig. 1 A, SIMS profile of sample 1 which exhibited the greatest cell efficiency V_{oc} and short circuit current I_{sc}. B, SIMS profile of sample 2. C, SIMS profile of sample 3. The cells exhibited the lowest efficiencies, fill factors and greatest R_s. D, SIMS profile of sample 4.

be orders of magnitude lower than the total concentration of impurities.

It is important to note that there were very high concentrations of impurities in the cell structures. Concentrations of carbon and chlorine were of the order 10^{19}–10^{20} atoms cm^{-3} throughout the CdTe layers, oxygen levels were greater (*ca.* by an order of magnitude). The absolute values at the surface are subject to question, as the secondary ion signals were unreliable in the transition region (which was estimated to be at 150 nm for each sample) before steady-state sputtering conditions were reached. One tentative conclusion that can be drawn from the SIMS profiles is that the CBD of CdS introduces high levels of carbonaceous species into the cell matrix.

The interface region between CdS and CdTe was characterised for all samples by a smooth tail in the sulfur profile extending into the CdTe substrate. The accurate profiling of an abrupt concentration gradient (*e.g.* a factor of 10 over 10 nm sputter depth) was not possible in this work due to the high primary ion beam energy. Interdiffusion results in an effective thinning of the CdS layer, which in turn suggests a minimum potentially critical thickness of CdS which must be employed in such devices. The effect of the formation of a Te-rich ternary *via* sulfur diffusion is to enhance the short wavelength response; the decrease in thickness of CdS leads to an increase in the long wavelength spectral response edge of the device.

It has been reported that the diffusion of sulfur in polycrystalline CdS/CdTe solar cells is similar for as-deposited and $CdCl_2$ treated materials. In contrast Te diffusion into CdS is reported to depend on post treatment, the formation of a ternary being negligible for chloride treated samples.[7] The extensive interdiffusion of layers observed for our CBD CdS/electrodeposited CdTe is in marked contrast to SIMS results obtained for CSS CdTe, for which compositional resolution near the interface is distorted by the roughness of the CdTe surface.[21] The maximum concentrations of carbon, chlorine and sulfur were found to coincide and we can tentatively ascribe this observation to impurity concentration at a depth of some 1600 nm into the matrix. Similar observations have been made by Dhere *et al.* but a direct comparison to their data is not possible as few experimental details were provided.[22]

A common feature for all samples was the location of the maximum of the oxygen concentration, some 150 nm closer to the SnO_2–F interface than peaks in the other profiles measured, which may suggest that the tin oxide layer provides a contribution to the high observed oxygen levels. Alternatively, the concentration of oxide impurities may be inherently greater in the CBD CdS layer due to its method of deposition. The nature of the ^{16}O profile may be also complicated by differential elemental sputtering.

The carbon signals were relatively noisy in comparison to those of the other isotopes investigated. This observation is consistent with the presence of particulate carbon within the matrix. Significant differences were observed for the carbon profiles of each sample. The greatest concentration of carbon was detected in sample 3 (Fig. 1C) with a maximum concentration ($\approx 7 \times 10^{19}$ atoms cm^{-3}) at a depth of 50 nm into the CdTe substrate. These cells had the largest R_s values (Table 5). Samples 2 and 3 (Fig. 1B and 1C) had similar profiles different to those for samples 1 and 4 (Fig. 1A and 1D). The latter had carbon impurities which were an order of magnitude lower (*i.e.* $\approx 10^{19}$ *vs.* $\approx 10^{20}$ atoms cm^{-3}) at the CdTe surface and were relatively consistent throughout the CdTe layer. The carbon profiles for all samples at the interface region were very similar.

Table 5 Photovoltaic cell characteristics of devices fabricated *via* CdS window materials from four different solution deposition baths. V_{oc} = open circuit voltage, I_{sc} = short circuit current, R_s = series resistance, R_p = shunt resistance, P_{max} = maximum power output, FF = fill factor

Cell bath no.	V_{oc}/V	I_{sc}/mA	R_s/Ω	R_p/Ω	P_{max}/mW	FF	Efficiency (%)
1	0.776	0.917	199	6710	0.408	0.574	7.8
2	0.750	0.709	268	8380	0.292	0.55	7.2
3	0.769	0.755	320	10400	0.300	0.517	6.9
4	0.769	0.747	294	7000	0.306	0.534	7.2

Cell efficiencies

The cell efficiencies (6.9–7.8%) and V_{oc} values (0.750–0.776 mV) were acceptable given the comparatively high concentrations of impurities (Table 5). It is interesting to compare the cell characteristics and respective isotopic profiles of the various devices studied. Sample 1 had values for I_{sc}, V_{oc}, FF and cell efficiency which were the best of all the devices examined. In contrast the worst R_s and cell efficiency values were determined for sample 3. The high R_s value for sample 3 is consistent with a device for which the bulk of the CdTe is poorly crystalline. The higher density of carrier recombination sites would be expected to result in poorer cell efficiencies. The recrystallisation of CdTe is known to be mediated by the presence of a chloride flux. The isotopic profiles of ^{12}C and ^{35}Cl in samples 1 and 3 are interesting, as the concentrations of carbon and chlorine in the CdTe bulk, *i.e.* beyond the interface region, are greater for sample 3 than for sample 1. We suggest that the higher concentration of carbon in sample 3 had an adverse effect upon the chloride diffusion and associated CdTe recrystallisation in sample 3. The relatively high V_{oc} for sample 3 appears to be inconsistent with the other cell characteristics, but V_{oc} is more indicative of the CdS : CdTe interface region, which suggests that recrystallisation at the heterojunction is successful but incomplete in the CdTe bulk.

Attempts were made to correlate CdS deposition bath chemistry with photovoltaic cell performance. We have outlined the possible association of high levels of carbonaceous material in the CdTe bulk with lower cell efficiencies. If we assume that the origin of the carbon impurity within cells, as determined by SIMS, is *via* the synthetic procedure (the C contamination cannot arise from the contacting procedure with evaporated Au) we would expect to find a relationship between cell efficiencies and the concentration of C-containing precursors in the CdS deposition baths. No simple association was found, *e.g.* cells derived from bath solution 4 (low solution pH and high concentration of thiourea) did not exhibit significantly poorer device performances. This negative result was interpreted as a reflection of the complicated interdependence of the processes of chloride diffusion, sulfur–tellurium interdiffusion, grain boundary migration and impurity/defect diffusion on cell performance.

The oxygen profiles will now be briefly discussed. For sample 1, the ^{16}O decreased from 10^{21} atoms cm^{-3} at the CdTe surface to a plateau at $\approx 5 \times 10^{19}$ atoms cm^{-3} in the bulk of the material, rising rapidly towards the interface region to a concentration of 2×10^{21} atoms cm^{-3}. In sample 2 a weak shoulder in the ^{16}O profile was apparent, centred at a depth of 450 nm from the surface of the CdTe substrate. The ^{16}O profile for sample 4 was highly uniform throughout the CdTe material ($\approx 2 \times 10^{19}$ atoms cm^{-3}) before reaching the interface region and CBD CdS layer.

The isotopic profiles for all samples indicate that the concentrations of ^{12}C, ^{35}Cl and ^{34}S appear to follow a similar distribution pattern at the CdTe–CdS interface region, although the absolute values differ. Similar observations have been reported.[23] It was most apparent that the levels of oxygen detected for all the samples under investigation could not be explained by a simple doping process. We can rationalise the observations as a consequence of the introduction of oxide material within the device, most probably as a result of the annealing processes (for both CdS and as-deposited cells) or alternatively *via* the tin oxide layer on the glass substrate.

Conclusion

Quantitative secondary ion mass spectrometry has been used to determine the elemental profiles and concentrations of isotopes ^{12}C, ^{16}O, ^{34}S and ^{35}Cl within n-CdS/p-CdTe thin film photovoltaic cells. High concentrations of ^{16}O, of the order 10^{20}–10^{21} atoms cm^{-3}, occur throughout all the cell structures and are consistent with the formation of oxide material during the post-deposition thermal processing and possibly with some contamination during the bath processing of CdS. Isotopic profiles of ^{12}C, ^{34}S and ^{35}Cl have similar maxima ($\approx 10^{19}$ atoms cm^{-3}) located at the CdS–CdTe interface. The development of the chloride rich interface region is a consequence of thermal treatment of both the CdS layer and the subsequent CdS–CdTe heterojunction device. Device characteristics are not obviously correlated with SIMS data. No simple relationship between CdS bath chemistry (*i.e.* reagent concentrations) and photovoltaic cell efficiency was found, but all the cells are of similar and modestly useful efficiency. The distribution of the carbon impurity that originates from the CdS chemical bath may influence both the chloride-promoted recrystallisation of CdTe and subsequent photovoltaic device characteristics. The latter association has not proven to be causal. These systems are in need of more study, however what is interesting is that cells of reasonable efficiency can be fabricated from materials which contain large amounts of impurities. The tolerance of these devices to impurities suggests that wet chemical methods may have great potential in the fabrication of large area/low cost photovoltaic cells.

Acknowledgements

The authors wish to thank Mr Richard Murphy of the National Microelectronics Research Centre (NMRC Ireland) for the provision of facilities and Dr Karl Senkiw (Department of Chemical Engineering, Imperial College) for the XPS analysis. This work was conducted under the Access to Large-Scale Facilities (LSF) European Community's Training and Mobility of Researchers (TMR) Programme. Paul O'Brien is the Sumitomo/STS Professor of Materials Chemistry and was the Royal Society Amersham International Research Fellow (1997–1998).

References

1 A. K. Turner, J. M. Woodcock, M. E. Özsan, D. W. Cunningham, D. R. Johnson, R. J. Marshall, N. B. Mason, S. Oktik, M. H. Patterson, S. J. Ransome, S. Roberts. M. Sadeghi, J. M. Sherborne, D. Sivapathasundaram and I. A. Wells, *Sol. Energy Mater. Sol. Cells*, 1994, **35**, 263.

2 L. D. Partain (editor), *Solar Cells and their Applications*, Wiley, New York, 1995; M. A. Green, *Solar Cells*, Prentice-Hall, New Jersey, 1982; T. L. Chu and S. S. Chu, *Solid-State Electron.*, 1995, **38**, 533.

3 J. M. Doña and J. Herrero, *J. Electrochem. Soc.*, 1997, **144**, 4081; J. Britt and C. Ferekides, *Appl. Phys. Lett.*, 1993, **62**, 2851; L. Stolt, J. Hedstrom, J. Kessler, M. Ruckh, K. O. Velthaus and H. W. Schock, *Appl. Phys. Lett.*, 1993, **62**, 597; T. L. Chu,

S. S. Chu, C. Ferekides, C. Q. Wu, J. Britt and C. Wang, *J. Appl. Phys.*, 1991, **70**, 7608.
4 A. C. Jones and P. O'Brien, *CVD of Compound Semiconductors; Precursor Synthesis, Development and Applications*, VCH, Weinheim, 1997; G. B. Stringfellow, *Organometallic Vapor Phase Epitaxy; Theory and Practise*, Academic Press, New York, 1989; *Chemical Beam Epitaxy and Related Techniques*, eds. G. J. Davies, J. S. Foord and W. T. Tsang, Wiley, Chichester, 1996; *Atomic Layer Epitaxy*, eds. T. Suntola and M. Simpson, Blackie, Glasgow, 1990.
5 P. O'Brien and T. Saeed, *J. Cryst. Growth*, 1996, **158**, 497.
6 Z. C. Feng, H. C. Chou, A. Rohatgi, G. K. Lim, A. T. S. Wee and K. L. Tan, *J. Appl. Phys.*, 1996, **79**, 2151; S. A. Galloway, P. R. Edwards and K. Durose, *Inst. Phys. Conf. Ser.*, 1997, **157**, 579.
7 W. Song, D. Mao, L. Feng, Y. Zhu, M. H. Aslan, R. T. Collins and J. H. Trefny, *Mater. Res. Soc. Symp. Proc.*, 1996, **426**, 331; H. C. Chou, A. Rohatgi, E. W. Thomas, S. Kamra and A. T. Bhat, *J. Electrochem. Soc.*, 1995, **142**, 254; T. L. Chu, S. S. Chu and A. T. Ang, *J. Appl. Phys.*, 1988, **64**, 1233.
8 K. Durose, P. R. Edwards and D. P. Halliday, *J. Cryst. Growth*, 1999, **197**, 733; A. Ringel, A. W. Smith, M. H. MacDougal and A. Rohatgi, *J. Appl. Phys.*, 1991, **70**, 881.
9 A. Kylner, J. Lindgren and L. Stolt, *J. Electrochem. Soc.*, 1996, **143**, 2662.
10 R. G. Wilson, F. A. Stevie and C. W. Magee, *Secondary Ion Mass Spectrometry: A Practical Handbook for Depth Profiling and Bulk Impurity Analysis*, Wiley, New York, 1989; A. Benninghoven, F. G. Rüdenauer and H. W. Werner, *Chemical Analysis*, Wiley, New York, Chichester, 1987, vol. 86.
11 J. Barker, S. Binns, D. Johnson, R. Marshall, S. Oktik, M. E. Özsan, M. Patterson, S. J. Ransome, S. Roberts, M. Sadeghi, J. M. Sherborne, A. Turner and J. Woodcock, *Int. J. Sol. Energy*, 1993, **12**, 79.
12 B. M. Basol, *Sol. Cells*, 1988, **23**, 69; G. C. Morris and S. K. Das, *IEEE Proc. 23rd Photovoltaic Specialists Conf., New York*, 1993, p. 469.
13 R. G. Wilson, *Int. J. Mass Spectrometry Ion Proc.*, 1993, **143**, 43.
14 R. Ortega-Borges and D. Lincot, *J. Electrochem. Soc.*, 1993, **140**, 3464; P. C. Rieke and S. B. Bentjen, *Chem. Mater.*, 1993, **5**, 43.
15 D. Briggs and M. P. Seah (Editors), *Practical Surface Analysis; Vol. 1 Auger and X-ray Photoelectron Spectroscopy*, Wiley, Chichester, 1992.
16 W. J. Danaher, I. E. Lyons and G. C. Morris, *Sol. Energy Mater.*, 1985, **12**, 137; A. Kylner and M. Wirde, *Jpn. J. Appl. Phys. Part 1*, 1997, **36(**4A), 2167.
17 D. S. Boyle, P. O'Brien, D. J. Otway and O. Robbe, *J. Mater. Chem.*, 1999, **9**, 725.
18 M. Stoev and A. Katerski, *J. Mater. Chem.*, 1996, **6**, 377.
19 K. Wittmaack, *Surf. Interface Anal.*, 1998, **26**, 290.
20 D. Briggs and M. P. Seah (Editors), *Practical Surface Analysis; Vol. 2 Ion and Neutral Spectroscopy*, Wiley, Chichester, 1992.
21 R. G. Dhere, K. Ramanathan, B. M. Keyes and H. R. Moutinho, *Proc. 12th Photovoltaic Program Review, Denver, CO, 1993, AIP Conf. Proc.*, 1993, **306**, 335.
22 R. G. Dhere, D. S. Albin, D. H. Rose, S. E. Asher, K. M. Jones, M. M. Al-Jassim, H. R. Moutinho and P. Sheldon, *Mater. Res. Soc. Symp. Proc.*, 1996, **426**, 361.
23 Y. Y. Loginov, K. Durose, H. M. Al-Allak, S. A. Galloway, S. Oktik, A. W. Brinkman, H. Richter and D. Bonnet, *J. Cryst. Growth*, 1995, **161**, 59.

Paper 9/04661E